Role of the N-terminal region in G protein-coupled receptor functions: negative modulation revealed by 5-HT2B receptor polymorphisms.

Arnauld Belmer, Stephane Doly, Vincent Setola, Sophie M. Banas, Imane Moutkine, Katia Boutourlinsky, Terry Kenakin, Luc Maroteaux

Title page

Role of the N-terminal region in G-protein coupled receptor functions: negative modulation revealed by 5-HT_{2B} receptor polymorphisms

Arnauld Belmer, Stephane Doly, Vincent Setola, Sophie M. Banas, Imane Moutkine, Katia Boutourlinsky, Terry Kenakin, and Luc Maroteaux

INSERM UMR S-839, Université Pierre et Marie Curie, Institut du Fer à Moulin, Paris, France (A.B., S.D., V.S., S.M.B., I.K., K.B., L.M.)

Department of Pharmacology, University of North Carolina School of Medicine, 120 Mason Farm Road, Room 4042, Genetic Medicine Building, CB 7365, Chapel Hill, North Carolina 27599-7365, USA (T.K.)

Running title page

Running title: N-terminus structural modulation of 5-HT_{2B} receptor

Correspondence should be addressed to: L Maroteaux; INSERM UMR S-839, Université Pierre et Marie Curie, Institut du Fer à Moulin, 17 rue du Fer à Moulin 75005 Paris, Tel 331 45 87 61 23 Fax 331 45 87 61 32 E-mail: luc.maroteaux@upmc.fr

Number of text pages, 34

Number of tables 1,

Number of figures, 7

Number of references, 29

Number of words in the *Abstract*, 247

Number of words in the *Introduction*, 535

Number of words in the *Discussion*, 1030

Supplementary data with 3 figures.

Nonstandard abbreviations.

α-methyl-5-(2-thienylmethoxy)-1*H*-indole-3-ethanamine hydrochloride (BW 723C86); seven transmembrane receptors (7TMRs); transmembrane (TM); serotonin (5-hydroxytryptamine, 5-HT); (±)-2,5-Dimethoxy-4-iodoamphetamine hydrochloride (DOI); Nor-(+)-Fenfluramine (NDF); (+)-Fenfluramine (DF); (±)-3,4Methylenedioxymethamphetamine (MDMA); Inositol Phosphate (IP); Dulbecco's Modified Eagle's Medium (DMEM); phosphate buffer saline (PBS); bovine serum albumine (BSA); wild type (WT); amino-acid (AA); N-terminal deletion of the first 32 AAs (ΔNter); phospholipase C (PLC); extracellular loop (ECL); Renilla luciferase (Rluc).

Abstract

Putative role of the N-terminal region of rhodopsin-like seven transmembrane biogenic amine receptors in agonist-induced signaling has not yet been clarified despite recent advances in seven transmembrane receptor structural biology. Given the existence of N-terminal non-synonymous polymorphisms (R6G;E42G) within the *HTR_{2B}* gene in a drug-abusing population, we assessed whether these polymorphisms affect 5-HT_{2B} receptor *in vitro* pharmacological and coupling properties in transfected COS-7 cells. Modification of the 5-HT_{2B} receptor N-terminus by the R6G;E42G polymorphisms, increases such agonist signaling pathways as inositol phosphate accumulation as assessed by either classical or operational models. The N-terminal R6G;E42G mutations of the 5-HT_{2B} receptor also increase cell proliferation and slow its desensitization kinetics compared to the wild type receptor, further supporting a role for the N-terminus in transduction efficacy. Furthermore, by co-expressing a tethered wild type 5-HT_{2B} receptor N-terminus with a 5-HT_{2B} receptor bearing a N-terminal deletion, we were able to restore original coupling. This reversion to normal activity of a truncated 5-HT_{2B} receptor by co-expression of the membrane-tethered wild type 5-HT_{2B} receptor N-terminus was not observed using a membrane-tethered 5-HT_{2B} receptor R6G;E42G N-terminus. These data suggest that the N-terminus exerts a negative control over basal as well as agonist-stimulated receptor activity that is lost in the R6G;E42G mutant. Our findings reveal a new and unanticipated role of the 5-HT_{2B} receptor N-terminus as a negative modulator, affecting both constitutive and agonist-stimulated activity. Moreover, our data caution against excluding the N-terminus and extracellular loops in structural studies of this seven transmembrane receptor family.

Introduction

The roles of the N-terminal region of seven transmembrane receptors (7TMRs) in receptor functions, such as ligand binding, surface expression, signaling, and desensitization, vary depending on the size and structure of the N-terminus. It is well established that in some 7TMRs, the N-terminus participates in cognate agonist binding and activation. These 7TMRs include secretin-like (family 2), metabotropic glutamate-like (family 3), and the rhodopsin-like (family 1) 7TMRs that bind peptides. Within this latter family, the N-terminal domain interaction with the core of the receptor has been associated with different modes of activation. For protease-activated receptors, cleavage of an N-terminal inhibitor initiates receptor activation (Ramachandran and Hollenberg, 2008). For glycoprotein hormone receptors, activation is dependent on the release of constitutive inhibition upon binding of a ligand to the N-terminus of the receptor (Vassart et al., 2004). For the melanocortin MC4R, a diffusible inverse agonist inhibits N-terminal activation (Ersoy et al., 2012; Srinivasan et al., 2004). However, the N-terminal regions of the rhodopsin-like 7TMR family interacting with such small ligands as monoamines have been the least studied among the superfamily, and their roles in agonist-induced signaling and desensitization have not been reported.

In some 7TMRs, such as the cannabinoid CB1 receptor, α1-adrenergic receptor, and GPR37, published data show that truncation of the N-terminal region increases plasma membrane expression of these receptors (Andersson et al., 2003; Dunham et al., 2009; Hague et al., 2004). The extracellular surface of biogenic amine 7TMRs affects ligand recognition, ligand 'escorting' into the binding pocket, and ligand binding kinetics (Wittmann et al., 2011). We previously observed that deletion of the long N-terminus of the *Drosophila* 5-HT_{2Dro} receptor (which most closely resembles the mammalian 5-HT_{2B} receptor) affects its pharmacology, with some compounds exhibiting a 10-fold change in affinity (Colas et al., 1997). This early finding suggested that the N-terminus affects the conformation of the

receptor transmembrane (TM) regions involved in ligand interactions, which may be relevant for receptor structure, because modelers usually exclude (often for technical reasons) 7TMR N-termini including the recently published crystal structures for 5-HT_{2B} receptors (Wacker et al., 2013). These observations suggested that the N-terminal regions of 7TMRs modulate the activity of biogenic amine 7TMRs by as-yet uncharacterized mechanisms.

Drug abuse vulnerability is a complex trait with strong genetic influences. Understanding the genetic bases of drug abuse vulnerability and particular allelic variants that contribute to this vulnerability can strongly improve our understanding of human addictions. We have recently extended the role of serotonin (5-hydroxytryptamine, 5-HT) in the behavioral responses to psychostimulants by revealing that the genetic ablation of *Htr_{2B}* in mice, the gene encoding 5-HT_{2B} receptors, eliminates locomotor response and place preference induced by (±)-3,4-methylenedioxymethamphetamine (MDMA) (Doly et al., 2009; Doly et al., 2008). Independently, three novel single nucleotide polymorphisms, two of which result in a point mutation, were described in a drug-abusing population (Lin et al., 2004). The Arg6, a conserved basic residue, and the conserved acidic Glu42 are mutated simultaneously into Gly, termed R6G;E42G.

Starting from these observations, the present work aimed to establish whether these polymorphisms within the 5-HT_{2B} receptor N-terminus affect receptor pharmacology. We discovered a new and unanticipated function of this extracellular region; *i.e.*, it acts as a negative structural modulator of receptor basal and stimulated activity.

Materials and Methods

Plasmid constructs- Human 5-HT_{2B} receptor cDNA was subcloned into the p513 vector, a derivative of the pSG5 mammalian expression vector (Green et al., 1988), which replicates in SV40 T antigen-transformed cells and drives 5-HT_{2B} receptor expression under the control of the SV40 early promoter. N-terminal variant 5-HT_{2B} receptors were generated using the Quickchange II (Stratagene, La Jolla, CA, USA) site-directed mutagenesis kit according to the manufacturer's protocol. The N-terminal truncated 5-HT_{2B} receptor mutant was generated by PCR deletion mutagenesis. TM1 constructs carrying different N-terminal sequence were obtained from each full construct by removing a PstI-PstI fragment (from AA85 to the C-terminal end of the 5-HT_{2B} receptor sequence).

TM1-tethered (WT, R6G;E42G or ΔNter) and ΔNter 5-HT_{2B} receptor coding regions were amplified from their respective cDNAs using appropriate sense and antisense primers. The fragments were then subcloned in frame in either a plasmid encoding C-terminus YFP (Clontech/BD Biosciences, Mountain View, CA) or Renilla luciferase (Rluc). The coding regions of all constructs were entirely sequenced. The Rluc construct was a kind gift from Stefano Marullo (U1016, Institut Cochin, Paris).

Cell culture- COS-7 cells were cultured as monolayers in Dulbecco's Modified Eagle's Medium (DMEM) (Gibco, Invitrogen, Carlsbad, CA, USA) supplemented with 10% fetal calf serum (Biowest) and 1% penicilin/streptomycin (Sigma, St Louis, MO, USA), in 9-cm dishes (*Falcon*). Cells were incubated at 37°C in a 5%CO_2 atmosphere. Cells were 80% confluent when transfected with 10µg of DNA using Nanofectin (PAA), according to the manufacturer's protocol, in an antibiotic-free medium. Four hours later, medium was replaced with fresh medium. Twenty-four hours after transfection, cells were incubated in serum free medium for membrane radioligand binding or trypsinized (Trypsin 1X 0.05% EDTA,

Invitrogen) and plated onto 24-well plates for IP accumulation and whole cell radioligand binding.

[^{3}H]Thymidine incorporation assay- Proliferation as measured by incorporation of radioactive desoxythymidine incorporation was performed as previously described (Deraet et al., 2005).

[^{3}H]Radioligands and drugs- [^{3}H]*Myo*-inositol (51.0 Ci/mmol), [^{3}H]-Mesulergine (99 Ci/mmol), [^{3}H]-5-Hydroxytryptamine (80.0 Ci/mmol) (5-HT), ^{125}I-(±)-2,5-Dimethoxy-4-iodoamphetamine hydrochloride (DOI) by Perkin Elmer, 5-hydroxytryptamine (5-HT), α-methyl-5-(2-thienylmethoxy)-1*H*-indole-3-ethanamine hydrochloride (BW 723C86), (±)-2,5-dimethoxy-4-iodoamphetamine hydrochloride (DOI) and nor-(+)-fenfluramine (NDF) by Sigma, (+)-fenfluramine (DF) by Tocris, mesulergine by RBI research; and (±)-3,4-methylenedioxymethamphetamine (MDMA) by Lipomed.

[^{3}H]Inositol Phosphate (IP) Accumulation Assay- Twenty-four hours before the experiment, cells were incubated in 24-well plates overnight with 20 nM of [^{3}H]*myo*-inositol diluted in an inositol-free medium (BME, Lonza, Basel, Switzerland). Just before receptor stimulation, medium was replaced by Krebs-Ringer-Hepes buffer (130 mM NaCl, 1.3 mM KCl, 2.2 mM $CaCl_2$, 1.2 mM NaH_2PO_4, 1.2 mM $MgSO_4$, 10 mM Hepes, 10 mM glucose, pH 7.4) supplemented with 20 mM LiCl to prevent IP_1 degradation. Cells were stimulated in duplicate in a final volume of 500 µl for 2 h. The experiment was stopped by replacing the stimulation medium with 10^{-3} M formic acid at room temperature for 20 min, and at 4°C overnight. Thus, IP_1 accumulated from IP_3 and IP_2 hydrolysis, was released from lysed and fixed cells. The accumulated IP_1 was eluted on anion exchange columns (Bio-Rad AG-1X8,

BioRad Laboratories, Hercules, CA, USA) with 0.2 M ammonium formiate in 0.1 M formic acid. Scintillation cocktail (Ultima Gold XR, Perkin Elmer) was added to the eluted [^{3}H]IP sample, and radioactivity was counted in a Beckman Coulter scintillation counter. At least three independent experiments were performed in duplicate, or in triplicate for tethered N-terminus experiments.

Desensitization Assay- To evaluate receptor desensitization, IP accumulation assays were performed as described above, except that a first agonist stimulation, in the absence of LiCl (to avoid IP accumulation), occurs at different time points (15, 30, 45, 60, 90 and 120 minutes) before a second stimulation with 100 nM of DOI. After the first stimulation, the medium was removed, the cells were washed three times with fresh medium, and fresh medium containing LiCl + DOI (100 nM) was added. The end of the experiment was carried out as previously described, and data were also normalized by each control condition, i.e. without the first stimulation (time 0 min). At least three independent experiments were performed in duplicate.

Membrane Radioligand Binding Assay- Membrane binding assays were performed on transfected cells plated in 9 cm dishes. Cells were first washed with PBS and scraped into 10 ml of PBS on ice, then centrifuged for 5 min at 1,000 *g*. Cell pellets were dissociated and lysed in 2 ml of binding buffer (50 mM Tris HCl, 10 mM $MgCl_2$, 0.1 mM EDTA, pH 7.4) and centrifuged for 30 min at 10,000 *g*. Membrane preparations were then resuspended in binding buffer to obtain a final concentration of 0.2-0.4 mg of protein/well. Aliquots of membrane suspension (200 µl/well) were incubated with 25 µl/well of [^{3}H] radioligand at a final concentration between half the K_D and the K_D for the 5-HT_{2B} receptor, diluted in binding buffer, and 25 µl/well of increasing concentrations of homologous compound (from 10^{-11} to

10^{-6} M, diluted in binding buffer) in 96-well plates for 90 min at room temperature. Membranes were harvested by rapid filtration onto Whatman GF/B glass fiber filters (Brandell) pre-soaked with cold saline solution and washed three times with cold saline solution to reduce non-specific binding. Filters were placed in 6-ml scintillation vials and allowed to dry overnight. The next day, 4 ml of scintillation cocktail were added to the samples, which were counted as before. Data in dpm were converted to fmoles and normalized to protein content (ranging from 0.1 to 0.5 mg/well). Specific binding represented 61.7±6.2% of maximal binding for heterologous and 52.0±3.8% for homologous competition of the maximal binding as determined in the presence of an excess of cold competitor. At least three independent experiments were performed in duplicate, (see **fig S1**).

Non-permeabilized Whole Cell Radioligand Binding Assay- Cells were plated in 24-well clusters. Twenty-four hours before the experiment, cells were incubated in serum-free medium overnight. The next day, medium was replaced by 400µl/well of Krebs-Ringer-Hepes buffer (130 mM NaCl, 1.3 mM KCl, 2.2 mM $CaCl_2$, 1.2 mM NaH_2PO_4, 1.2 mM $MgSO_4$, 10 mM Hepes, 10 mM Glucose, pH 7.4). Then, 50 µl of tritium-labeled compounds were diluted in Krebs-Ringer-Hepes buffer at a final concentration between half the K_D and the K_D for the 5-HT_{2B} receptor. The tritriated radioligand was competed with 50 µl of increasing concentrations of non-radioactive ligand, also diluted in Krebs-Ringer-Hepes buffer. Cells were then incubated for 30 min (5-HT_{2B} receptor) at room temperature and then washed twice on ice with cold phosphate-buffered saline (PBS). Washed cells were solubilized by addition of 500 µl of SDS 1%. The next day, 4 ml of scintillation cocktail were added to the samples, and the radioactivity was counted using a scintillation counter (Beckman Coulter). Data in dpm were converted to fmoles and normalized to protein content (0.2-0.4 mg of protein/well). Specific binding represented 44.2±2.1% for heterologous and 44.5±5.3% for homologous

competition of the maximal binding as determined in the presence of an excess of cold competitor. At least three independent experiments were performed in duplicate, (see **fig S1**).

Immunocytochemistry- COS-7 cells plated on coverslips after transfection with either the wild type (WT) TM1-N-terminus (TM1-WT), TM1-R6G;E42G or TM1-ΔNter constructs fused to YFP together with 5-HT_{2B} receptor ΔNter were incubated overnight in serum-free DMEM before immunocytochemistry experiments. Then, cells were washed three times with cold PBS and fixed for 15 min with 4% paraformaldehyde. After three washes with PBT + bovine serum albumin (BSA) 3%, cells were incubated at room temperature for 4 h with an antibody against the C-terminus of the 5-HT_{2B} receptor (1:1000). After three washes with PBT+BSA (3%), the primary antibody was revealed by a 1-h incubation with a donkey anti-mouse antibody coupled to CY3 (1:1000). After three washes, coverslips were mounted with Mowiol. Similar experiments were performed after transfection with TM1-N-terminus (TM1-WT) alone. After three washes with PBS + bovine serum albumin (BSA) 3% without permeabilization, cells were incubated at room temperature for 4 h with a rabbit antibody against the N-terminus of the 5-HT_{2B} receptor (1:1000) (Pharmingen). After three washes with PBS+BSA (3%), the primary antibody was revealed by a 1-h incubation with a goat-anti-rabbit antibody coupled to Alexa 488 (1:1000). After three washes, coverslips were mounted with Mowiol.

For coimmunoprecipitation experiments, Flag-tagged wild-type 5-HT2B and YFP-tagged TM1 constructs were transfected in COS-7 cells. After forty eight hours, cells were washed in PBS, sonicated and solubilized in lysis buffer [75 mM Tris, 2 mM EDTA, 12 mM MgCl2, 10 mM CHAPS, protease inhibitor cocktail EDTA free, pH 7.4] during 5 hours at 4°C. Lysates were centrifuged at 12,000 g during 30 min at 4°C. Immunoprecipitations were performed using EZview Red FLAG M2 Affinity Gel (Sigma) according to manufacturer's

recommendations. Immunoprecipitated proteins and 50 µg of total proteins were combined with Laemmli buffer, heated at 70°C for 10 min and run on Nupage 4-12% Bis-Tris gel (LifeTechnologies). Immunoblots were probed with anti-gfp (Roche) or anti-flag (Sigma) antibodies diluted 1/2000 and immunoreactivity was revealed using secondary antibody coupled to 680nm fluorophores using the Odyssey LI-COR infrared fluorescent scanner.

BRET assays- Bioluminescence Resonance Energy Transfer (BRET) assays were performed according to published methods (Achour et al., 2011). Briefly, COS-7 cells (5×10^5 per well of a 6-well plates) were transfected with 30 ng plasmid DNA coding for the BRET donor (ΔNter 5-HT_{2B}-Luc) and increasing amounts of BRET acceptor plasmids (TM1-tethered WT, R6G;E42G or ΔN-ter-YFP; 100-4000 ng per well) or YFP. Twenty-four hours after transfection, cells were washed in PBS, detached using 10 mM EDTA in PBS, centrifuged (1400g for 5 minutes), resuspended in Hank-balanced salt solution and distributed in 96-well plates (PerkinElmer plates; 10^5 cells per well). After addition of the luciferase substrate, coelenterazine h (5 µM final concentration), luminescence and fluorescence were measured simultaneously (at 485 and 530 nm, respectively) in a Mithras LB940 plate reader. The BRET ratio was calculated as: ([emission at 530 nm/emission at 485 nm] – [background at 530 nm/background at 485 nm]), where background corresponds to signals in cells expressing the Rluc fusion protein alone under the same experimental conditions. For better readability, results were expressed in milli-BRET units (mBRET), 1 mBRET corresponding to the BRET ratio multiplied by 1000. BRET ratios were plotted as a function of ([YFP-YFP0]/YFP0)/(Rluc/Rluc0), where YFP is the fluorescence signal at 530 nm after excitation at 485 nm, and Rluc the signal at 485 nm after addition of coelenterazine h. YFP0 and Rluc0 correspond to the same values in cells expressing the Rluc fusion protein alone.

Data analysis- Binding data were analyzed using the iterative non-linear regression model (GraphPad Prism 6.0). This allowed the calculation of inhibition constants (K_i) and the maximal number of sites (B_{max}). All values represent the average of independent experiments ± SEM (n = number of experiments as indicated in the text). For IP coupling experiments, data obtained in dpm were analyzed using Graphpad Prism, converted to fmoles, and normalized to protein content and receptor B_{max} (obtained in whole cell radioligand binding experiments of the same transfected cells). A single dose-response experiment may not accurately determine affinity and efficacy since a drug that binds with high affinity but has low efficacy will produce the same dose-response curve as a drug with low affinity and high efficacy. To untangle affinity from efficacy, we used the operational model initially described by (Black and Leff, 1983), which defines response as:

$$\text{Response} \quad A = [A]^n \tau^n E_m / [A]^n \tau^n + ([A] + K_A)^n \quad (1)$$

where E_m represents the maximal response capability of the system, K_A is the equilibrium dissociation constant of the agonist–receptor complex, n is the slope of the dose–response curve and τ is the efficacy. This final term represents the receptor density and molecular interaction of the agonist– receptor complex interaction with the stimulus–response system of the cell, which itself has ligand-specific elements (efficacy of the ligand) and system-specific elements (efficiency of coupling of receptors to signalling pathway). A theoretically complete term to describe the power of a ligand to active a cellular pathway is the term τ/K_A; this incorporates both elements of efficacy and affinity. Considering that the most common difference between systems is receptor density, ratios of τ/K_A account for these and should be system-independent measures of the relative power of ligands to activate pathways.

Another useful measure of agonist activity is Ehlert's "activity ratio" (denoted RA). Both affinity and efficacy for a single number of agonism for dose–response curves of unit slope have been solved with the application of relative activity (RA) ratios. Proposed by Ehlert and

colleagues (Ehlert, 2005), the RA value is the maximal response of the agonist divided by the EC50. This furnishes a single number reflecting the power of a molecule to produce agonism in any system. In terms of the maximal response and EC_{50} for dose– response curves in the Black Leff operational model (Black and Leff, 1983), it can be shown that RA represents the relation:

$$RA = \tau^n ((2 + \tau^n)^{1/n} - 1) E_m / K_A (1 + \tau^n) \quad (2)$$

For dose–response curves of unit slope (n = 1), it can be seen that RA reduces to the term $E_m(\tau/K_A)$. Ratios of these terms for particular agonists cancel the E_m term and are therefore system independent. Values of τ/K_A have the added advantage of circumventing another issue with full agonists, namely the fact that an infinite variety of combinations of efficacy and affinity can describe any given curve to a full agonist (there is no unique value of efficacy that can be identified unless the curve indicates partial agonism). The Δlog(RA) values were calculated as: Δlog(RA)agonist/reference = log(RA)agonist - log(RA)reference to compare various agonists within signaling pathway. The Δlog(RA) values were calculated as: Δlog(RA)R6G;E42G/wild type = Δlog(RA)R6G;E42G - Δlog(RA)wild type. The ΔΔlog(RA) values provided a scale to compare partial agonist (DOI) and reference full agonist (5-HT) between the wild-type and mutant R6G;E42G receptor. The bias ($10^{\Delta\Delta\log(RA)}$) represent the signaling difference between the wild-type and mutant receptor for the specific coupling pathway, here the IP coupling, for DOI relative to 5-HT. The calculations of 95% confidence intervals were made with the program Mathematica 5.0 (Kenakin et al., 2012).

Statistics- Comparisons between groups were performed using Student's unpaired *t* test or one- or two-way ANOVA with Bonferroni's posthoc test were used depending on the experiment. Significance was set at $p < 0.05$.

Results

The N-terminus of the 5-HT_{2B} receptor affects agonist affinity.

Starting from the report by Lin et al. (Lin et al., 2004), we explored the pharmacological properties of the R6G;E42G variant 5-HT_{2B} receptor, which contains two amino acid (AA) changes in the N-terminal region (**Fig. 1**). To study the effect of the N-terminal mutations, we compared wild type (WT) and variant 5-HT_{2B} receptor-transfected COS-7 cells using radioligand binding assays. Homologous competition experiments showed a left shift in the displacement curve for 5-HT binding (**Fig. 2a**). The 5-HT_{2B} variant receptor had a five-fold increase in affinity for 5-HT; *i.e.*, a five-fold decrease in the K_i for the R6G;E42G ($p < 0.05$) variant relative to the WT receptor (**Table 1**). Using the 5-$HT_{2B/2C}$ receptor-selective agonist BW723C86 as a competitor, a four-fold increase in affinity was found compared to WT receptor (**Table 1**). A similar effect was observed using the 5-HT_2 agonist DOI as a competitor, which displayed a 2.4-fold increase in affinity for the N-terminal variant receptor compared to the WT. Because none of the tested antagonists were affected by the SNPs (**Table 1- Fig. 2b**), it was likely that the mutations affect receptor coupling. However, the fact that only some of the tested agonists are affected by this variant may be related to a probe dependence issue, agonism being a combined interaction of the modulator (agonist), receptor and signaling protein, known to be probe dependent. Nevertheless, this gain of affinity seems independent of the type of agonism, full agonists being not differentially affected compared to partial agonists (**Table 1-** Cussac et al., 2008). In light of the finding that N-terminal deletion of the 5-HT_{2Dro} affected the affinity of some agonists (Colas et al., 1997), we tested the effect of N-terminal deletion the first 32 AAs of the human 5-HT_{2B} receptor (**Fig. 1**) (ΔNter). Interestingly, this N-terminal truncation generated an apparent shift in agonist affinity, with a 30-fold increase in affinity for 5-HT (**Fig. 2a**). Because the R6G;E42G variant results in neutralization of two oppositely charged AA side chains, we hypothesized that these residues

interacted electrostatically. Based on this, we tested whether exchanging the position of the charged residues would alter 5-HT_{2B} receptor ligand affinity vis-à-vis the WT receptor. Thus, we generated the 'charge swap' mutant R6E;E42R. This inversion also increased its apparent affinity for 5-HT (**Fig. 2a**), indicating that a missing electrostatic interaction in the R6G;E42G variant likely affects its pharmacological properties.

The N-terminus of the 5-HT_{2B} receptor can modulate receptor-Gαq activation.

We then explored the impact of N-terminal modifications on an immediate effector of 5-HT_{2B} receptors, the Gαq/11–sensitive membrane phospholipase C (PLC). Upon agonist binding, the 5-HT_{2B} receptor stimulates hydrolysis of membrane phosphatidyl inositol-bisphosphate (PIP_2) into cytoplasmic inositol phosphates (IP_3, which promotes intracellular calcium release, and the degradation products IP_2 and IP_1) and diacylglycerol (an activator of protein kinase C) (Deraet et al., 2005). Since the N-terminal mutations may affect cell surface expression, we evaluated the cell surface expression as receptor B_{max} using tritiated mesulergine competition comparing purified membrane to non-permeabilized whole cells binding (**Supplemental Fig. 1**). Only a fraction of the total membrane binding capacity was found on whole cells, supporting the rationale to used whole cell B_{max} as an estimate of surface receptor to normalize coupling efficiency.

Integrating these B_{max} values to normalize for surface receptor expression, increasing concentrations of a partial 5-HT_2 agonist, DOI, activated the R6G;E42G variant more efficaciously than the WT receptor, leading to a increase of both minimal (E_{min} +48%) and maximal (E_{max} +56%) cytoplasmic IP accumulation, as well as activation efficiency (E_{max}-E_{min}), with little effect on apparent agonist potency EC_{50} (**Fig. 2c**). The N-terminal deletion of the first 32 AAs (ΔNter) also generated an increase in IP basal activity (ΔNter 68%). DOI also induced a stronger 5-HT_{2B} receptor-mediated IP accumulation as did basal 5-HT_{2B} receptor-

mediated PIP_2 hydrolysis, with a noticeable increase for the ΔNter mutant (ΔNter 97%), while the inverse mutant displayed a moderate increase in E_{max} (15%) (**Fig. 2c**). This basal activity was tested against a known inverse agonist for the receptor, ritanserin, which was able to reverse this basal activity to similar extent (**Supplemental Fig. 2a**). Other tested agonists followed the same trend as DOI, activating the R6G;E42G variant receptor more efficaciously than the WT receptor (+25% for 5-HT, $p < 0.05$; +17% for dexfenfluramine - DF, $p < 0.01$; +20% for nordexfenfluramine - NDF, $p < 0.05$; +21% for DOI, $p < 0.001$ and +30% for MDMA, $p < 0.05$) (**Supplemental Fig. 2b-e**). Taken together, these results indicate that the human R6G;E42G polymorphism leads to increased coupling of the 5-HT_{2B} receptor to phospholipase C activity. Notably, the IP responses for the R6G;E42G variant were significantly increased for DOI as well as for other agonists including MDMA, DF, and its metabolite NDF.

Validation using the operational model of the modulation by the N-terminus of the 5-HT_{2B} receptor-Gαq activation.

To take into account putative alteration of the efficiency of receptor coupling, which may vary among the mutants, we used the Black-Leff operational model to derive Ehlert's "activity ratio" (denoted RA) (Ehlert, 2005), the RA value is the maximal response of the agonist divided by the EC50 and calculate putative difference in signaling characteristics for IP production for each mutant as ΔΔLog(RA) (Black and Leff, 1983; Ehlert, 2005; Kenakin et al., 2012). Using ΔΔLog(RA) values and comparing two agonist probes (5-HT as full agonist and DOI as partial agonist) for each receptor species, cancels all effects of the measurement, i.e. expression level, assay coupling etc..., simply revealing differences in the way the two probes (agonists) interact with the receptor conformation. Differences in Log(RA) values are informing about intrinsic differences in the receptor conformation (See **Data Analysis**

Section, Fig. 3a,b,c, and supplemental Fig. 3). The data shows that the R6G;E42G and R6E;E42R mutations produced significant differences in the relative way 5-HT and DOI bind to and active the receptor. These show statistically significant differences between the relative activity of 5-HT and DOI produced by the R6G;E42G mutation (DOI was more active when compared to 5-HT) (**Fig. 3c**). The R6E;E42R mutation (DOI was relatively less active when compared to 5-HT) and the ΔNter mutation produced little effect in the way 5-HT and DOI interact (or at the least, the changes induced by the mutation are the same for both probes) (**Supplemental Fig. 3**).

So far, the results obtained by two independent approaches support a role for the N-terminus variant R6G;E42G in controlling the efficacy and affinity of DOI-stimulated 5-HT_{2B} receptor-mediated PIP_2 hydrolysis, suggesting that the two AA substitutions encoded by this polymorphism are sufficient to modify N-terminal function over the receptor.

Validation of N-terminal domain interactions

Further evidence for the involvement of the 5-HT_{2B} N-terminus in receptor function was obtained using dual genetic constructs: the first TM domain of the 5-HT_{2B} receptor (TM1) was used as a membrane tether for various N-terminal sequences and was co-transfected with N-terminally truncated receptors (**Fig. 4a-i**) to explore putative intermolecular (*in trans*) effects. The underlying hypothesis was that expression of the TM1-tethered WT N-terminus could interact and thus suppress the effect of N-terminal truncation on receptors by direct interactions.

In order to first validate putative interactions between TM1-tethered construct and 7TMR, COS-7 cells were cotransfected with plasmids coding for ΔNter 5-HT_{2B} receptor and TM1-tethered (WT, R6G;E42G or ΔNter)-YFP. Confocal analysis using a 5-HT_{2B} receptor antibody revealed colocalization with the YFP for all tested TM1-tethered (WT, R6G;E42G

or ΔNter-YFP) construct (**Fig 4a-i**). This observation supports the putative close localization between these different receptor fragments upon co-expression. Proper membrane expression of the TM1-tethered N-terminus was also verified by immunofluorescence and confocal microscopy on non-permeabilized cells using an antibody raised against the N-terminus of the human 5-HT_{2B} receptor (**Fig. 4j,k**).

To validate putative interactions between the TM1-tethered construct and N-terminally truncated 5-HT_{2B} receptor, COS-7 cells were then cotransfected with plasmids encoding ΔNter 5-HT_{2B} receptor-FLAG and TM1-tethered (WT, R6G;E42G or ΔNter)-YFP or free YFP (negative controls). Western blot of proteins immunoprecipitated with anti-FLAG antibody and probed with GFP antiserum indicated that all tested TM1-tethered (WT, R6G;E42G or ΔNter)-YFP constructs co-immunoprecipitated with 5-HT_{2B} receptor-FLAG but not with YFP (**Fig 5A-D**). This result further supports protein-protein interactions between the various receptor constructs.

Interactions between TM1-tethered (WT, R6G;E42G or ΔNter) constructs and ΔNter 5-HT_{2B} receptor were further examined in living COS-7 cells using bioluminescence resonance energy transfer (BRET). ΔNter 5-HT_{2B} receptor fused to Rluc (ΔNter 5-HT_{2B}-Luc) was expressed in the presence of increasing concentrations of BRET acceptors, consisting of TM1-tethered WT, R6G;E42G or ΔNter linked to cytoplasmic YFP. In all cases, hyperbolic saturation curves were obtained, further supporting protein-protein interactions (**Fig 5E-H**). BRET signals markedly depend on the relative distance of donor and acceptor, explaining why maximal BRET values were slightly different (57.20±5.33 ; 67.44±2.93 ; 61.9±7.3). The value of the YFP:Luc ratio at which half-maximal BRET was obtained was comparable, indicating that these three TM1 constructs displayed the same propensity to associate with ΔNter 5-HT_{2B}-Luc (1.30±0.44 ; 0.86±0.15 ; 0.96±0.33). Free YFP was used as negative

control; only a linear nonspecific BRET signal was obtained confirming the specificity of the observed interactions.

Functional impact of N-terminal domain interactions

We then evaluated the functional impact receptors measured through the average E_{min} and E_{max} for IP accumulation after DOI stimulation first for the WT receptor (**Fig. 6A**) after correction for the protein input and for the surface receptor B_{max}. We evaluated similarly E_{max} for IP accumulation after DOI stimulation of each combination of constructs (**Fig 6B**). When co-transfected with a WT 5-HT_{2B} receptor, the different TM1-tethered 5-HT_{2B} receptor N-terminal constructs did not modify IP levels compared to the WT control alone. In addition, when the R6G;E42G receptor was co-transfected with a TM1-tethered ΔNter construct lacking the N-terminal 32 amino acids of the 5-HT_{2B} receptor or a TM1 construct carrying the WT N-terminus (TM1-WT), IP accumulation was increased up to 129% of agonist-induced WT level, as previously described for the variant receptor alone and taking into account the surface expression of this mutant. Thus, neither the WT nor the truncated N-terminal TM1 construct (TM1-WT or TM1-ΔNter) did modify the increase in IP levels induced by the R6G;E42G variant. The increase in IP levels was also significant in the chimeric construct totally lacking any N-terminal fragment (ΔNter + TM1-ΔNter), as previously observed for the ΔNter receptor. However, when a TM1 construct carrying the WT N-terminus (TM1-WT) was co-transfected with the ΔNter receptor, intracellular IP accumulation was significantly decreased, becoming non-significantly different from WT level (**Fig. 6C**). However, IP accumulation was still increased (>130% WT level) when the ΔNter receptor was co-transfected with a TM1 construct carrying the variant mutation (TM1-R6G;E42G). This result indicates that tethered expression of a WT N-terminus (TM1-WT) is able to restore the WT activity *in trans* (**Fig. 6C**). Although able to interact biochemically, the lack of effect for the

TM1-tethered R6G;E42G fragment clearly demonstrates the loss of N-terminus functionality in the variant receptor.

Functional impact of N-terminal domain variant on other transduction pathways.

In addition to IP coupling, we previously showed that the 5-HT_{2B} receptor can activate cell proliferation via both Gαq/11 and Gα13 (Deraet et al., 2005). We therefore assessed whether the polymorphism in the N-terminal sequence modifies the proliferative function of the 5-HT_{2B} receptor as measured by [^{3}H]thymidine incorporation (**Fig. 7A**). Interestingly, in response to 1 μM 5-HT, COS-7 cells expressing the R6G;E42G variant incorporated five times more thymidine than did cells transfected with WT receptor. This observation suggests that the 5-HT_{2B} N-terminus is important for additional effector pathways including proliferation.

Finally, we observed that the gain-of-function dual SNP altered the desensitization process of the receptor. We evaluated the desensitization kinetics of the receptor variant by first challenging with DOI in the absence of LiCl (no IP accumulation) and then, after extensive washing, repeating the DOI challenge at various time points in the presence of LiCl. As shown in **Figure 7B**, the receptor variant desensitized more slowly than did the WT receptor, consistent with a modified signal transduction capacity of the polymorphic 5-HT_{2B} receptor.

Discussion

We report a functional study of two *HTR_{2B}* SNPs that modify two amino acids (R6G;E42G) within the N-terminus of the receptor. The polymorphisms were previously identified in drug-abusing patients. We show that the R6G;E42G variant of the 5-HT_{2B} receptor displays increased agonist affinity and efficacy, as highlighted by an increased basal activity E_{min} and increased E_{max} of agonist-induced IP production after normalization by protein content and cell surface receptor expression Bmax or in the black-Leff operational model. Furthermore, this variant also increases the ability of the receptor to trigger cell proliferation and leads to decreased desensitization kinetics.

Historically, rhodopsin-like 7TMRs have been identified and studied on the basis of their ability to be activated by high-affinity diffusible pharmacological ligands interacting directly with the core transmembrane region of the receptor. Interestingly, we found in this study that R6G;E42G 5-HT_{2B} receptors are more efficiently coupled to G proteins than are WT receptors, as shown by agonist binding and functional assays. Using various TM1-tethered N-termini co-expressed with ΔNter receptor, we demonstrate that these TM1-tethered N-termini can interact with the 7TM domains using complementary approaches: colocalization in fixed cells, coimmunoprecipitation in solubilized lysates, and BRET experiments on living cells. Furthermore, when the ΔNter receptor was co-transfected with a TM1 construct carrying the WT N-terminus, coupling was reversed to WT levels, indicating that tethered expression of a WT N-terminus was able to reverse the gain of coupling due to the deletion of the N-terminus from the 5-HT_{2B} receptor. This was not observed when the ΔNter receptor was co-transfected with a TM1 construct carrying the variant mutation (TM1-R6G;E42G). Thus, the N-terminus can alter the coupling efficiency of the receptor *in trans*.

Structural basis of 7TMR oligomerization have been recently obtained in β1-adrenergic receptors (Huang et al., 2013). In an inactive conformation, two dimer interfaces were

identified: one involving TM1, and the other engaging residues from TM4 and TM5 (Huang et al., 2013). Previous findings using biochemical approaches have identified similar interactions in 5-HT_{2C} receptors (Mancia et al., 2008). It is thus not totally surprising that, using TM1-tethered N-terminal constructs, we found direct interactions with the 7TM receptor. However, the fact that these interactions were able to modulate basal and agonist-stimulated receptor activity was not anticipated. Recently solved crystal structures have directly confirmed previous findings that biogenic amine 7TMRs including 5-HT_{2B} receptors bind endogenous ligands within the TM helical bundle of the receptor (Manivet et al., 2002; Setola et al., 2005; Wacker et al., 2013). Conventional agonists target the same binding site on a receptor as the endogenous ligand, termed the orthosteric site (Smith et al., 2011). Our results support the view that the 5-HT_{2B} receptor N-terminus, by interacting with TM and/or extracellular loops, acts negatively on coupling efficiency in both basal and stimulated conditions without directly interfering with the orthosteric site. Thus, we propose that the 5-HT_{2B} receptor N-terminus behaves as a negative structural modulator of the receptor activation. The fact that the R6G;E42G variant also increases the ability of the receptor to trigger cell proliferation and leads to a decreased desensitization kinetic indicates that this modulation acts generally on the receptor activation process, rather than specifically affecting certain intracellular signaling pathways.

These findings extend those of previous studies that have demonstrated a role for the N-terminus in the function of rhodopsin-like 7TMRs. An interaction between the N-terminus and the ECL3 of CXCR4 and C5aR has also been implicated in an activation micro-switch region: whereas the N-terminus/ECL3 interaction stabilizes the active state of CXCR4, it acts as an inverse agonist in C5aR, possibly by making multiple contacts with the TM domains to stabilize the inactive state (Rana and Baranski, 2010). Furthermore, the N-terminus of histamine H1 receptors interacts with the ECL2 to influence receptor pharmacology by

contributing to ligand binding, receptor activation, and agonist selectivity (Strasser et al., 2008). Since the publication of the β2-adrenergic receptor crystal structure, a number of new 7TMR homology models based on this template have been reported. Accurate prediction of the loops, particularly those surrounding the orthosteric binding site, remains one of the more difficult aspects in 7TMR homology modeling. In a previous report of homology models, 5-HT_{2B} receptors were identified as presenting difficulty in modeling their ECL2 (McRobb et al., 2010). This has been solved by the recently published crystal structure for the 5-HT_{2B} receptor (Wacker et al., 2013). The E212-R213-F214 residues of the 5-HT_{2B} receptor form an additional helical turn stabilized by a structured water molecule at the extracellular tip of helix V (Wacker et al., 2013). As a result, the segment of ECL2 that connect helices III and V via the conserved disulfide bond is shortened in the 5-HT_{2B} receptor. However, the N-terminus being absent in this crystal structure, further investigations are necessary to fully understand the interactions of the N-terminus with the ECLs/TMs of 5-HT_{2B} receptors.

The N-terminal regions of 7TMRs have been shown to control the surface expression of receptor proteins, but their effects vary depending on the structural features of each receptor. Polymorphisms in the β2-adrenergic receptor (R16G;Q27E) display normal agonist binding and functional coupling to Gs, but markedly alter the degree of agonist-promoted down-regulation of receptor expression (Green et al., 1994). In human β1-adrenergic receptor, the N-terminal G49 variant was found to display a more profound agonist-promoted down-regulation and both basal and agonist-stimulated adenylyl cyclase activity than the S49 variant (Levin et al., 2002). Here, we show that the increased basal and agonist-stimulated IP activity, gain of function in R6G;E42G receptor coupling is associated with a reduced rate of receptor desensitization, which may participate to this gain of function.

Our study further revealed that not only signal transduction pathways but also desensitization kinetic could be affected by modifying the N-terminus of 5-HT_{2B} receptors.

Although *in vivo* validation of these findings have to be performed, it is clear that our findings support the need for modeling 7TMR with their N-terminus and extracellular loops in order to fully understand their activation mechanisms. In conclusion, by using deletion or mutation that leads to a gain of coupling efficiency both in basal and stimulated conditions, our results support that the human 5-HT_{2B} receptor N-terminus behaves as a negative modulator of the receptor activity.

Acknowledgements

We thank Jean-Marie Launay for helpful discussions and for critical reading of this manuscript and Stefano Marullo for Rluc plasmid and advices on BRET experiments.

Authorship Contributions.

Participated in research design: A Belmer, S Doly, V Setola and L Maroteaux.

Conducted experiments: A Belmer, S Doly, S Banas, V Setola, I. Moutkine and K Boutourlinsky.

Performed data analysis: A Belmer, S Doly, S Banas, V Setola and L Maroteaux.

Wrote or contributed to the writing of the manuscript: A Belmer, S Doly, V Setola, T Kenakin and L Maroteaux.

References

Achour L, Kamal M, Jockers R and Marullo S (2011) Using quantitative BRET to assess G protein-coupled receptor homo- and heterodimerization. *Methods Mol Biol* **756**:183-200

Andersson H, D'Antona AM, Kendall DA, Von Heijne G and Chin CN (2003) Membrane assembly of the cannabinoid receptor 1: impact of a long N-terminal tail. *Mol Pharmacol* **64**(3):570-577

Black JW and Leff P (1983) Operational models of pharmacological agonism. *Proc R Soc Lond B Biol Sci* **220**(1219):141-162

Colas J-F, Choi D-S, Launay J-M and Maroteaux L (1997) Evolutionary conservation of the 5-HT2B receptors. *New York Acad Science* **812**:148-150

Cussac D, Boutet-Robinet E, Ailhaud MC, Newman-Tancredi A, Martel JC, Danty N and Rauly-Lestienne I (2008) Agonist-directed trafficking of signalling at serotonin 5-HT2A, 5-HT2B and 5-HT2C-VSV receptors mediated Gq/11 activation and calcium mobilisation in CHO cells. *Eur J Pharmacol* **594**(1-3):32-38

Deraet M, Manivet P, Janoshazi A, Callebert J, Guenther S, Drouet L, Launay JM and Maroteaux L (2005) The natural mutation encoding a C terminus-truncated 5-Hydroxytryptamine2B receptor is a gain of proliferative functions. *Mol Pharmacol* **67**(4):983-991

Doly S, Bertran-Gonzalez J, Callebert J, Bruneau A, Banas SM, Belmer A, Boutourlinsky K, Herve D, Launay JM and Maroteaux L (2009) Role of serotonin via 5-HT2B receptors in the reinforcing effects of MDMA in mice *PLoS ONE* **4**(11):e7952

Doly S, Valjent E, Setola V, Callebert J, Herve D, Launay JM and Maroteaux L (2008) Serotonin 5-HT2B receptors are required for 3,4-methylenedioxymethamphetamine-

induced hyperlocomotion and 5-HT release in vivo and in vitro. *J Neurosci* **28**(11):2933-2940

Dunham JH, Meyer RC, Garcia EL and Hall RA (2009) GPR37 surface expression enhancement via N-terminal truncation or protein-protein interactions. *Biochemistry* **48**(43):10286-10297

Ehlert FJ (2005) Analysis of allosterism in functional assays. *J Pharmacol Exp Ther* **315**(2):740-754

Ersoy BA, Pardo L, Zhang S, Thompson DA, Millhauser G, Govaerts C and Vaisse C (2012) Mechanism of N-terminal modulation of activity at the melanocortin-4 receptor GPCR. *Nat Chem Biol* **8**:725-730

Green S, Issemann I and Sheer E (1988) A versatile in vivo and in vitro eukaryotic expression vector for protein engineering. *Nucl Ac Res* **16**:396

Green SA, Turki J, Innis M and Liggett SB (1994) Amino-terminal polymorphisms of the human beta 2-adrenergic receptor impart distinct agonist-promoted regulatory properties. *Biochemistry* **33**(32):9414-9419

Hague C, Chen Z, Pupo AS, Schulte NA, Toews ML and Minneman KP (2004) The N terminus of the human alpha1D-adrenergic receptor prevents cell surface expression. *J Pharmacol Exp Ther* **309**(1):388-397

Huang J, Chen S, Zhang JJ and Huang X-Y (2013) Crystal structure of oligomeric β1-adrenergic G protein-coupled receptors in ligand-free basal state. *Nat Struct Mol Biol* **20**(4):419-425

Kenakin T, Watson C, Muniz-Medina V, Christopoulos A and Novick S (2012) A simple method for quantifying functional selectivity and agonist bias. *ACS Chem Neurosci* **3**(3):193-203

Levin MC, Marullo S, Muntaner O, Andersson B and Magnusson Y (2002) The myocardium-protective Gly-49 variant of the beta 1-adrenergic receptor exhibits constitutive activity and increased desensitization and down-regulation. *J Biol Chem* **277**(34):30429-30435

Lin Z, Walther D, Yu X-Y, Drgon T and Uhl GR (2004) The human serotonin receptor 2B: coding region polymorphisms and association with vulnerability to illegal drug abuse. *Pharmacogenetics* **14**(12):805-811

Mancia F, Assur Z, Herman AG, Siegel R and Hendrickson WA (2008) Ligand sensitivity in dimeric associations of the serotonin 5HT2c receptor. *EMBO Rep* **9**(4):363-369

Manivet P, Schneider B, Smith JC, Choi DS, Maroteaux L, Kellermann O and Launay JM (2002) The serotonin binding site of human and murine 5-HT2B receptors: molecular modeling and site-directed mutagenesis. *J Biol Chem* **277**:17170-17178

McRobb FM, Capuano B, Crosby IT, Chalmers DK and Yuriev E (2010) Homology modeling and docking evaluation of aminergic G protein-coupled receptors. *J Chem Inf Model* **50**(4):626-637

Ramachandran R and Hollenberg MD (2008) Proteinases and signalling: pathophysiological and therapeutic implications via PARs and more. *Br J Pharmacol* **153 Suppl 1**:S263-282

Rana S and Baranski TJ (2010) Third extracellular loop (EC3)-N terminus interaction is important for seven-transmembrane domain receptor function: implications for an activation microswitch region. *J Biol Chem* **285**(41):31472-31483

Setola V, Dukat M, Glennon RA and Roth BL (2005) Molecular determinants for the interaction of the valvulopathic anorexigen norfenfluramine with the 5-HT2B receptor. *Mol Pharmacol* **68**(1):20-33

Smith NJ, Bennett KA and Milligan G (2011) When simple agonism is not enough: emerging modalities of GPCR ligands. *Mol Cell Endocrinol* **331**(2):241-247

Srinivasan S, Lubrano-Berthelier C, Govaerts C, Picard F, Santiago P, Conklin BR and Vaisse C (2004) Constitutive activity of the melanocortin-4 receptor is maintained by its N-terminal domain and plays a role in energy homeostasis in humans. *J Clin Invest* **114**(8):1158-1164

Strasser A, Wittmann HJ and Seifert R (2008) Ligand-specific contribution of the N terminus and E2-loop to pharmacological properties of the histamine H1-receptor. *J Pharmacol Exp Ther* **326**(3):783-791

Vassart G, Pardo L and Costagliola S (2004) A molecular dissection of the glycoprotein hormone receptors. *Trends Biochem Sci* **29**(3):119-126

Wacker D, Wang C, Katritch V, Han GW, Huang XP, Vardy E, McCorvy JD, Jiang Y, Chu M, Siu FY, Liu W, Xu HE, Cherezov V, Roth BL and Stevens RC (2013) Structural features for functional selectivity at serotonin receptors. *Science* **340**(6132):615-619

Wittmann H-J, Seifert R and Strasser A (2011) Influence of the N-terminus and the E2-loop onto the binding kinetics of the antagonist mepyramine and the partial agonist phenoprodifen to H(1)R. *Biochem Pharmacol* **82**(12):1910-1918

Footnotes

Source of financial support.

These studies were supported by the Centre National de la Recherche Scientifique, the Institut National de la Santé et de la Recherche Médicale, the Université Pierre et Marie Curie, and by grants from the Fondation de France, the French Ministry of Research Agence Nationale pour la Recherche [ANR-12-BSV1-0015-01], S. D. was supported by a Lefoulon-Lalande fellowship, A. B. by a Société Française de Pharmacologie Thérapeutique fellowship and V. S. by a Marie Curie EU fellowship, and L.M.'s team is part of the École des Neurosciences de Paris Ile-de-France network and of the Bio-Psy Labex.

Reprint requests should be addressed to L Maroteaux; INSERM UMR S-839, Université Pierre et Marie Curie, Institut du Fer à Moulin, 17 rue du Fer à Moulin 75005 Paris,

Tel 331 45 87 61 23

Fax 331 45 87 61 32

E-mail: luc.maroteaux@upmc.fr

V. S. present address: West Virginia University School of Medicine Department of Physiology and Pharmacology, Robert C. Byrd Health Sciences Center, 1 Medical Center Drive Morgantown, West Virginia 26506 USA

A. B. and S. D. are equal contributors

Legends for Figures

Figure 1: Molecular description of the 5-HT_{2B} receptor. Amino acid sequence and localization of the variant R6G;E42G in the N-terminus of 5-HT_{2B} receptor. The known 5-HT binding site residues are presented in dark grey circles with black letters. The R6G;E42G variant substitution position is presented in red circles with white letters and the R6E;E42R inverted variant in light blue with black letters on the N-terminal sequence. Double arrowhead locates the N-terminus deletion (ΔNter).

Figure 2: Pharmacological characterization of the R6G;E42G variant of human 5-HT_{2B} receptor. A. Representative example of [^{3}H]-5-HT radioligand binding homologous competition experiments performed on membrane preparation of COS-7 cells transfected with plasmids encoding the WT, the R6G;E42G, the R6E;E42R, and the ΔNter receptors showing a left shift in the ΔNter, the R6E;E42R and the R6G;E42G variant receptors curve (Ki of 3.34±0.76, 1.08±0.60, 2.34±0.79, 0.107±0.016 nM, Bmax of 560±30, 240±70, 420±75, 120±25 fmoles/mg prot for WT, R6G;E42G, R6E;E42R, and ΔNter, respectively). Representative result of 5 independent experiments each performed in triplicate, (see **Table 1** for compete results). **B**. Homologous antagonist competition binding (Mesulergine) shows no difference between cells transfected with WT, R6G;E42G or ΔNter 5-HT_{2B} receptors. **C.** Dose-response of agonist-induced IP accumulation of COS-7 cells transfected with plasmids encoding the WT, ΔNter, R6G;E42G and R6E;E42R receptors stimulated for 2 hours with increasing concentrations of DOI (from 10^{-9} to 10^{-5} M). Calculated EC50 revealed very little impact of the different mutations on apparent coupling efficiency (31±11, 18±12, 37±10, 34±7 nM for WT, ΔNter, R6E;E42R, and R6G;E42G respectively). Representative result of at least 3 independent experiments each performed in duplicate, normalized in fmoles of IP per fmoles of surface receptors, i.e. corrected by whole cells B_{max} and statistically analyzed by

two-way ANOVA repeated measures with mutation and drug concentration as main factors; effect of mutations on IP accumulation, $F(3,24) = 148.35$ $p < 0.0001$. A Bonferroni post tests was also applied on each graph, statistical significance: **, P< 0.01, ****, P< 0.0001 vs. WT receptor.

Figure 3: Black-Leff operational model to derive putative bias in coupling of variant receptor. To take into account efficiency of receptor coupling, which may vary among the mutants, we used the Black-Leff operational model to calculate putative difference in signaling characteristics for IP production for each mutant as ΔΔLog(RA). We used 2 agonist probes (5-HT as full agonist and DOI as partial agonist) to cancel putative impact of receptor density differences. DOI- and 5-HT-stimulated IP dose response curves are shown for COS-7 cells transfected with plasmids encoding the WT receptor (**A**) and the R6G;E42G (**B**). Using 5-HT and DOI as probes of the 2 receptor types, there was a difference produced in the relative activity of 5-HT and DOI with the mutation from WT to R6G;E42G (**C**). This is demonstrated by the ΔΔLog(RA) value 95% confidence limits. There was a significant increase in the relative activity of DOI over 5-HT produced by the mutation (Bias of 1.23). Results for 5-HT (full reference agonist and DOI as partial agonist) are expressed in fmoles of IP accumulation (n=3 independent experiments performed in duplicate).

Figure 4: Confocal microscopy images of transfected COS-7 cells showing colocalization of 5-HT_{2B}-ΔNter and various TM1 constructs. COS-7 cells were co-transfected with expression vectors encoding 5-HT_{2B}-ΔNter (**a–i**) and TM1-WT-YFP (**a-c**), or TM1-R6G/E42G-YFP (**d-f**), or TM1-ΔNter-YFP (**g-i**) and analyzed by confocal immunofluorescence microscopy. **a, d and g** Green staining from the transfected TM1-YFP. **b, e and h** Red staining (Cy3) from 5-HT_{2B}-ΔNter revealed using mouse monoclonal

antibody directed toward C-terminus of the receptor. **c, f and i** Merge shows colocalization of the signal in yellow. **j, k.** In order to ensure that the TM1 construct were also able to reach plasma membrane, we performed immunostaining of TM1-WT construct without the YFP fusion protein. Antibodies against the N-terminus of the 5-HT_{2B} receptor were incubated without permeabilization indicating that the TM1-WT construct were indeed able to be expressed at the cell surface ; non-transfected cells are shown as a negative control for immunoreactivity. a-i bar = 5µM; jk bar = 25µM.

Figure 5: TM1-tethered (WT, R6G;E42G or ΔNter) interaction with ΔNter 5-HT_{2B} receptor. A-D: Immunoprecipitation of TM1-tethered (WT, R6G;E42G or ΔNter) with ΔNter 5-HT_{2B} receptor. COS-7 cells were cotransfected with plasmids coding for 5-HT_{2B} receptor-flag (2B-flag) and TM1-tethered (WT, R6G;E42G or ΔNter -YFP) or free YFP (negative controls). Representative western blots are shown of 3 independent immunoprecipitation experiments. **A** Direct blot of input of proteins revealed using flag antibody; **B** Direct blot of input of proteins revealed using GFP antibody; **C** Blot of immunoprecipitated proteins using the flag antibody and revealed with the flag antiserum. **D** Blot of immunoprecipitated proteins using the flag antibody and revealed with the GFP antiserum. **E-H: BRET analysis of TM1-tethered (WT, R6G;E42G or ΔNter) interaction with ΔNter 5-HT_{2B} receptor**. COS-7 cells were cotransfected with plasmids coding for ΔNter 5-HT_{2B} receptor-Rluc (the BRET donor) and increasing concentrations of TM1-tethered (WT, R6G;E42G or ΔNter-YFP, the BRET acceptors) or free YFP (negative controls). Energy transfer was measured after addition of the membrane permeable luciferase substrate coelenterazine h. The BRET signal was determined by calculating the ratio of light emitted at 530 nm over the light emitted at 485 nm. The value of the YFP:Luc ratio, for which half-maximal BRET obtained, was comparable, indicating that these 3 forms of TM1 display

the same propensity to associate with ΔNter 5-HT_{2B} receptor. Representative BRET saturation curves are shown of 3 independent experiments. Error bars indicate SEM of specific BRET-ratio values obtained from triplicate.

Figure 6: Functional study of different variants of 5-HT_{2B} receptors. A. Basal IP accumulation (E_{min}) of COS-7 cells transfected with plasmids encoding the WT, the R6G;E42G, the R6E;E42R and the ΔNter receptors. B_{max} for WT, the R6G;E42G, the R6E;E42R, and the ΔNter receptors are 982±84, 784±102, 860±74, 508±100 fmoles/mg of proteines, respectively. **B.** DOI-stimulated IP maximum (E_{max}) accumulation of COS-7 cells transfected with plasmids encoding the WT, the R6G;E42G, the R6E;E42R, and the ΔNter receptors stimulated with DOI (1 µM). Results are presented as percent of WT level from 3 independent experiments each performed in duplicate that were normalized in fmoles of IP per fmoles of surface receptors per mg of protein, i.e. corrected by protein and cell surface B_{max}. Typical full dose response curve is shown on fig 2c. Statistical analysis was done by Welch-corrected t-test. n= 3-5 independent experiments performed at least in duplicate. (Statistical significance: ****, P< 0.0001 vs. WT receptor). **C**. Functional study of different variants of 5-HT_{2B} receptors co-expressed with a TM1-tethered N-terminus. TM1-WT and TM1-R6G;E42G constructs are 93 amino acids long and TM1-ΔNter construct is deleted of the 32 first amino acids, i.e. 61 amino acids long. The IP accumulation was measured after DOI (1 µM) stimulation of COS-7 cells transfected with plasmids encoding the WT, variant (R6G;E42G) and ΔNter receptors. Results were normalized in fmoles of IP per fmoles of surface receptors per mg of protein, i.e. corrected by protein and cell surface B_{max} and then to WT level and were statistically analyzed by one-way ANOVA and Bonferroni's multiple comparison post test. $F_{(7, 64)} = 6.83$ $p < 0.0001$, n=3 independent experiments each performed in triplicate. (Statistical significance: *: P<0.05, **: P<0.01 vs. WT+TM1-ΔNter; #: P<0.05,

##: P<0.01 vs. WT+TM1-WT; §: P<0.05, §§: p<0.01 vs. WT+TM1-R6G;E42G; $: P<0.05 vs. ΔNter+TM1-ΔNter; £: P<0.05 vs. ΔNter+TM1- R6G;E42G). B_{max} for the WT+TM1ΔNter, WT+TM1WT, WT+TM1R6G;E42G, the R6G;E42G+TM1ΔNter, R6G;E42G+TM1WT, and the ΔNter+TM1ΔNter, ΔNter+TM1WT, ΔNter+TM1R6G;E42G receptors are 769±306, 800±345, 767±309, 686±278, 667±224, 554±256, 643±321, 585±266 fmoles/mg of proteins, respectively.

Figure 7: Proliferation rate of R6G;E42G 5-HT_{2B} receptor compared to WT 5-HT_{2B} receptors. a. Measurement of proliferation rate by [^{3}H] thymidine incorporation performed for COS-7 cells transfected with plasmids encoding the WT receptor and for the variant R6G;E42G. Thymidine levels are normalized to WT. Results of 4 independent experiments each performed in triplicate were statistically analyzed by Unpaired t test with Welch's correction (****, P< 0.0001). **b.** Desensitization kinetics was evaluated after a first stimulation with 100 nM of DOI replaced by fresh medium containing LiCl + DOI (100 nM). A delay of desensitization of the R6G;E42G variant receptor was observed during the first 30 minutes, compared to WT. Results of experiments performed in duplicate were statistically analyzed by two-way ANOVA analysis of variance with mutation and time as main factors; effect of mutations on desensitization, $F(1,2) = 19.35$ $p = 0.048$. A Bonferroni post tests was also applied on each graph, statistical significance: *, P< 0.05; **, P< 0.01 vs. WT receptor.

Table 1:

Affinity constants (pKi) for different agonist and antagonist compounds binding to R6G;E42G 5-HT$_{2B}$ receptor compared to WT 5-HT$_{2B}$ receptors.

		pKi (mean ± SEM)		Statistical analysis
		WT	R6G;E42G	Two tailed t-test
Agonists vs. [^{3}H] 5-HT	5-HT	8.41 ± 0.11	9.05 ± 0.18	P = 0.0162
vs. [^{125}I] DOI	mCPP	7.80 ± 0.05	7.87 ± 0.07	NS
	MK212	7.00 ± 0.08	6.89 ± 0.10	NS
	Ro 60.0332	7.78 ± 0.06	7.93 ± 0.06	NS
	DOI	7.64 ± 0.04	8.03 ± 0.05	P = 0.0003
	BW 723C86	7.82 ± 0.03	8.46 ± 0.07	P < 0.0001
	Ro 60.0175	9.30 ± 0.08	9.23 ± 0.11	NS
	norDF	8.67 ± 0.09	8.95 ± 0.04	NS
	5-HT	8.25 ± 0.05	8.87 ± 0.07	P < 0.0001
Antagonists vs. [^{125}I] DOI	Lisuride	8.95 ± 0.06	8.92 ± 0.06	NS
	Ro 60.0869	7.97 ± 0.12	8.05 ± 0.05	NS
	RS 10.2221	6.70 ± 0.04	6.58 ± 0.10	NS
	SB 24.2084	7.36 ± 0.06	7.41 ± 0.14	NS
	Ketanserin	6.57 ± 0.03	6.34 ± 0.13	NS
	Mesulergine	8.66 ± 0.06	8.69 ± 0.08	NS
	SB 20.6553	8.13 ± 0.09	8.42 ± 0.13	NS
	Mianserin	8.15 ± 0.04	8.31 ± 0.12	NS
	Ritanserin	8.81 ± 0.05	9.03 ± 0.10	NS
	SB 21.5505	8.89 ± 0.06	8.92 ± 0.06	NS
	SB 20.4741	7.17 ± 0.05	7.33 ± 0.11	NS
	LY 26.6097	9.51 ± 0.05	9.63 ± 0.09	NS
	RS 127.445	9.44 ± 0.04	9.28 ± 0.05	NS
	MDL 100.907	5.96 ± 0.05	5.87 ± 0.06	NS
vs. [^{3}H] Mesulergine	Mesulergine	8.51 ± 0.08	8.44 ± 0.05	NS
	RS 127.445	9.07 ± 0.13	8.93 ± 0.15	NS

Pharmacological determinations were performed on transiently transfected COS-7 cells expressing the relevant receptor by homologous or heterologous competition. Values are presented as mean ± SEM, n=5 independent experiments, each performed in triplicate.

Figure 1

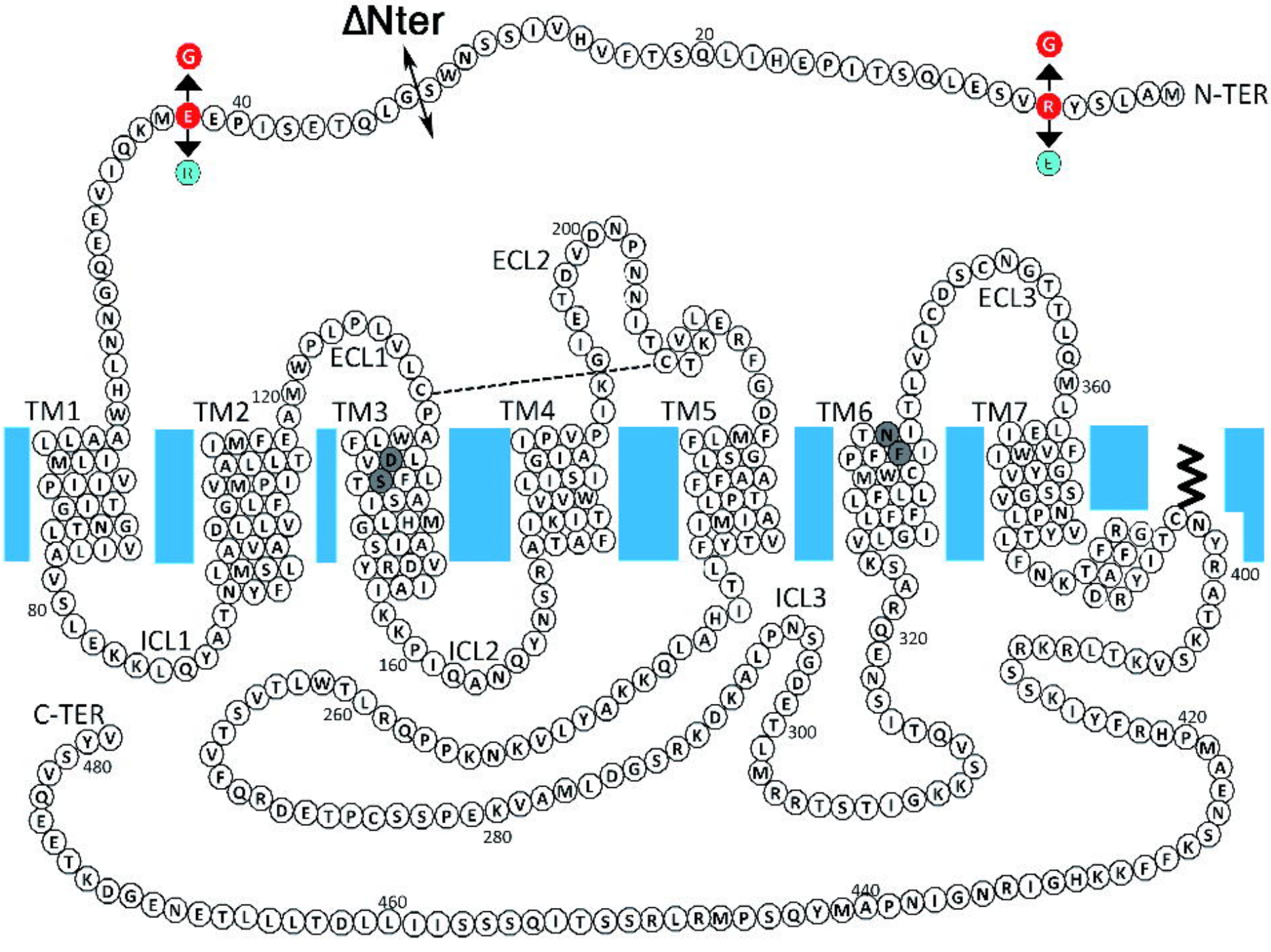
ΔNter
N-TER
C-TER
TM1
TM2
TM3
TM4
TM5
TM6
TM7
ECL1
ECL2
ECL3
ICL1
ICL2
ICL3

Figure 2

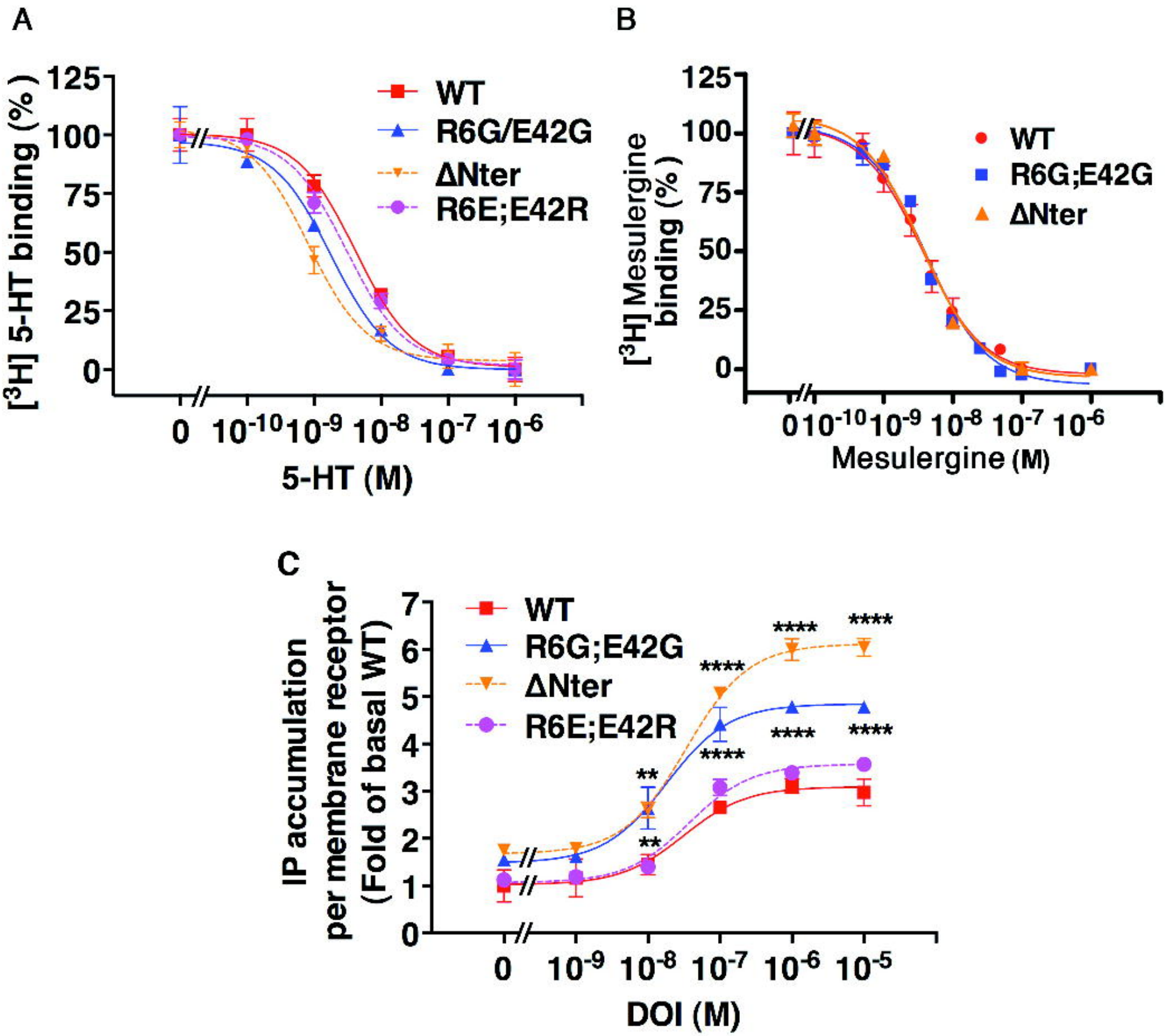
A
[3H] 5-HT binding (%)
125
100
75
50
25
0
WT
R6G/E42G
ΔNter
R6E;E42R
0 10-10 10-9 10-8 10-7 10-6
5-HT (M)
B
[3H] Mesulergine binding (%)
125
100
75
50
25
0
WT
R6G;E42G
ΔNter
0 10-10 10-9 10-8 10-7 10-6
Mesulergine (M)
C
IP accumulation per membrane receptor (Fold of basal WT)
7
6
5
4
3
2
1
0
WT
R6G;E42G
ΔNter
R6E;E42R
**
**
****
****
****
****
****
0 10-9 10-8 10-7 10-6 10-5
DOI (M)

Figure 3

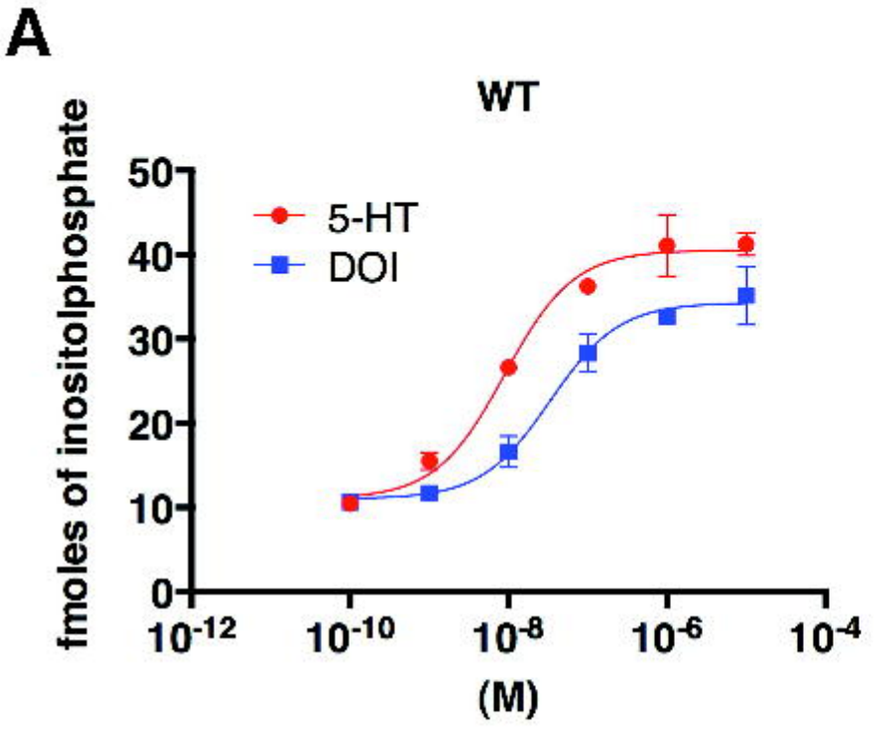

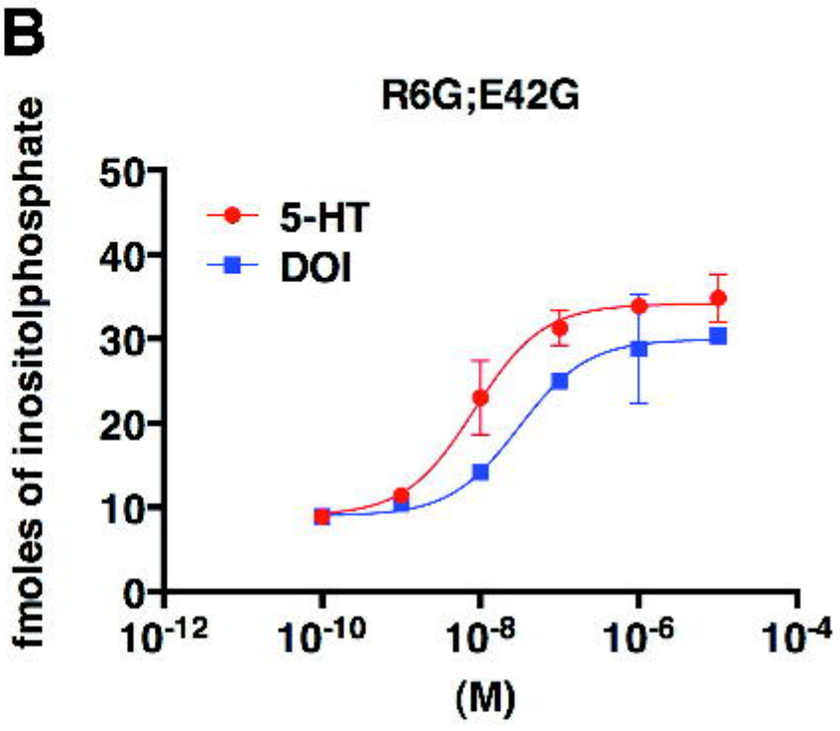

C

	WT		R6G;E42G	
	5-HT Log(RA)	DOI Log(RA)	5-HT Log(RA)	DOI Log(RA)
	8.119	7.535	8.075	7.67
	8.048	7.69	8.274	7.73
	8.156	7.575	8.349	8.04
mean ±95% c.l.	8.108 8.13 to 8.08	7.6 7.62 to7.57	8.23 8.26 to 8.21	7.81 7.84 to 7.79
Δlog(RA) ± 95% c.l.	0.508 0.545 to 0.471		0.42 0.455 to 0.384	

ΔΔLog(RA) +95% c.l.	0.088 0.11 to 0.067
BIAS= 1.23	

Figure 4

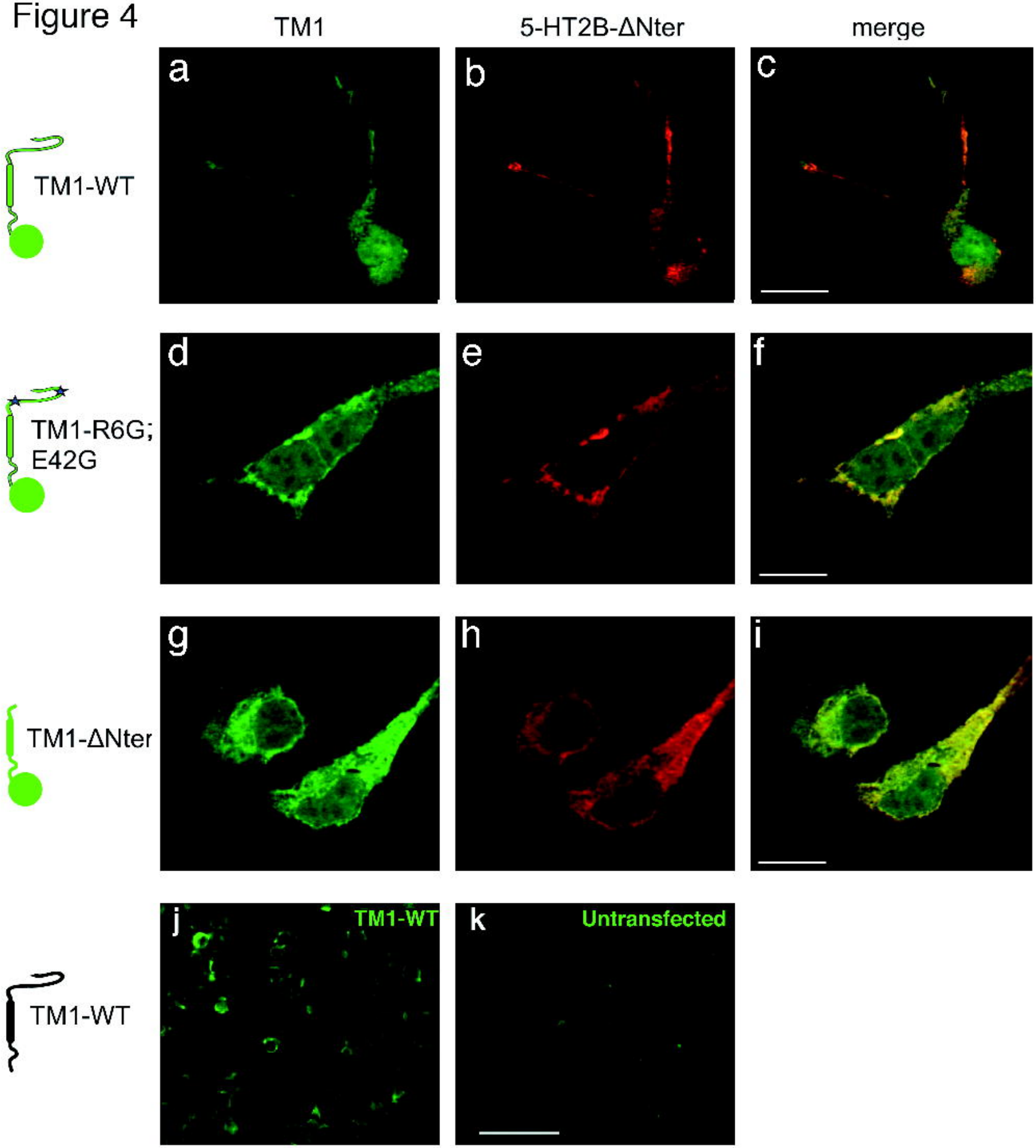
TM1
5-HT2B-ΔNter
merge
a
b
c
TM1-WT
d
e
f
TM1-R6G;
E42G
g
h
i
TM1-ΔNter
j
TM1-WT
k
Untransfected
TM1-WT

Figure 5

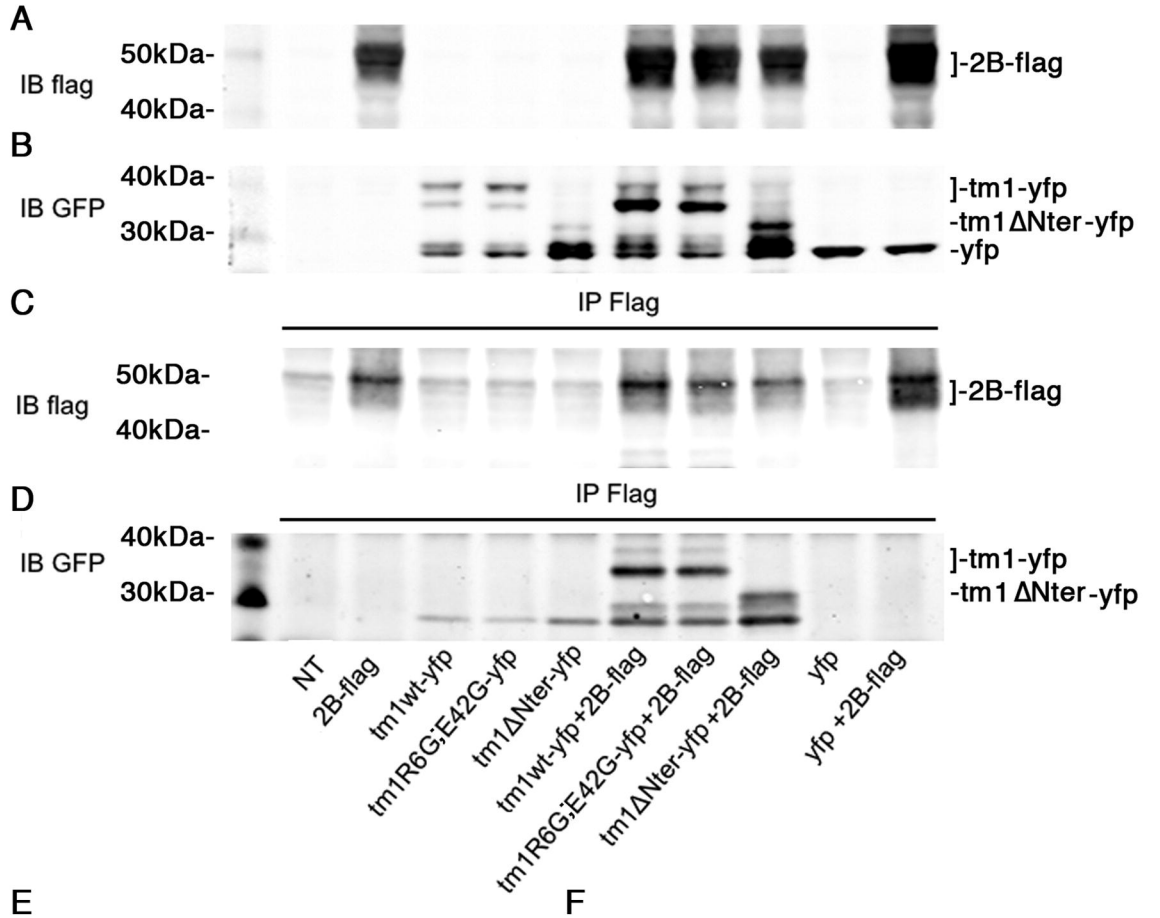
A
IB flag
50kDa-
40kDa-
]-2B-flag
B
IB GFP
40kDa-
30kDa-
]-tm1-yfp
-tm1ΔNter-yfp
-yfp
C
IP Flag
IB flag
50kDa-
40kDa-
]-2B-flag
D
IP Flag
IB GFP
40kDa-
30kDa-
]-tm1-yfp
-tm1 ΔNter-yfp
NT
2B-flag
tm1wt-yfp
tm1R6G;E42G-yfp
tm1ΔNter-yfp
tm1wt-yfp+2B-flag
tm1R6G;E42G-yfp+2B-flag
tm1ΔNter-yfp+2B-flag
yfp
yfp +2B-flag

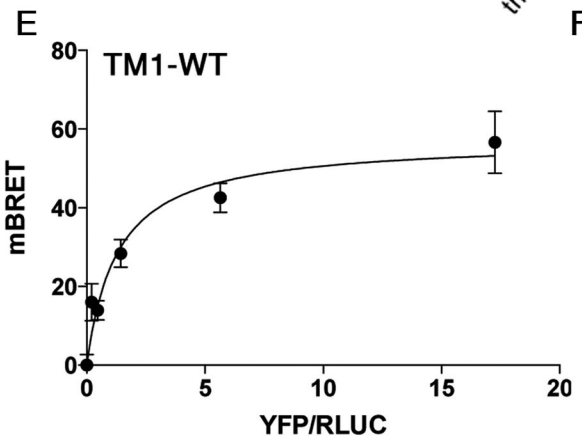
E
TM1-WT
mBRET
YFP/RLUC
0
20
40
60
80
0
5
10
15
20

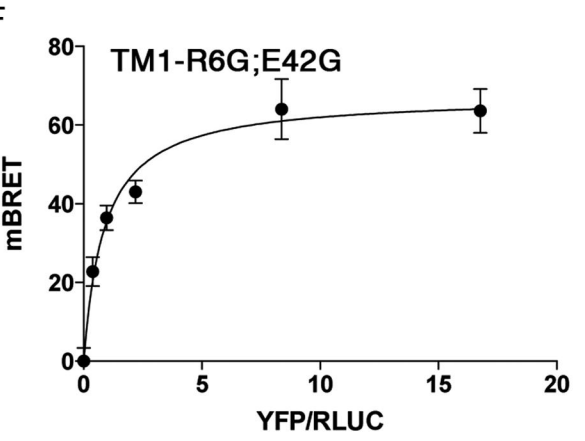
F
TM1-R6G;E42G
mBRET
YFP/RLUC
0
20
40
60
80
0
5
10
15
20

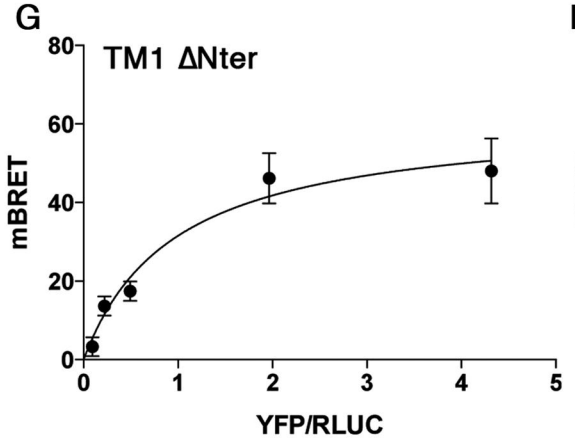
G
TM1 ΔNter
mBRET
YFP/RLUC
0
20
40
60
80
0
1
2
3
4
5

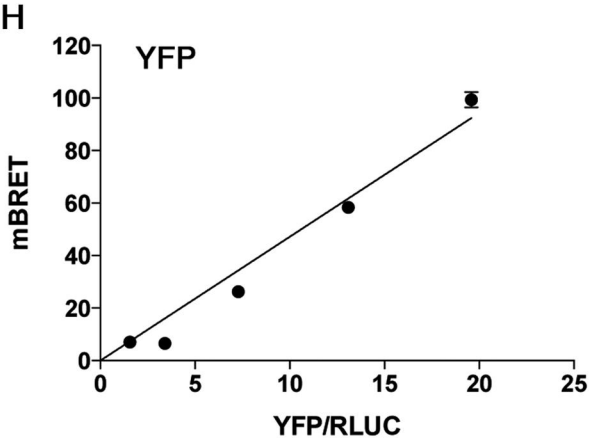
H
YFP
mBRET
YFP/RLUC
0
20
40
60
80
100
120
0
5
10
15
20
25

Figure 6

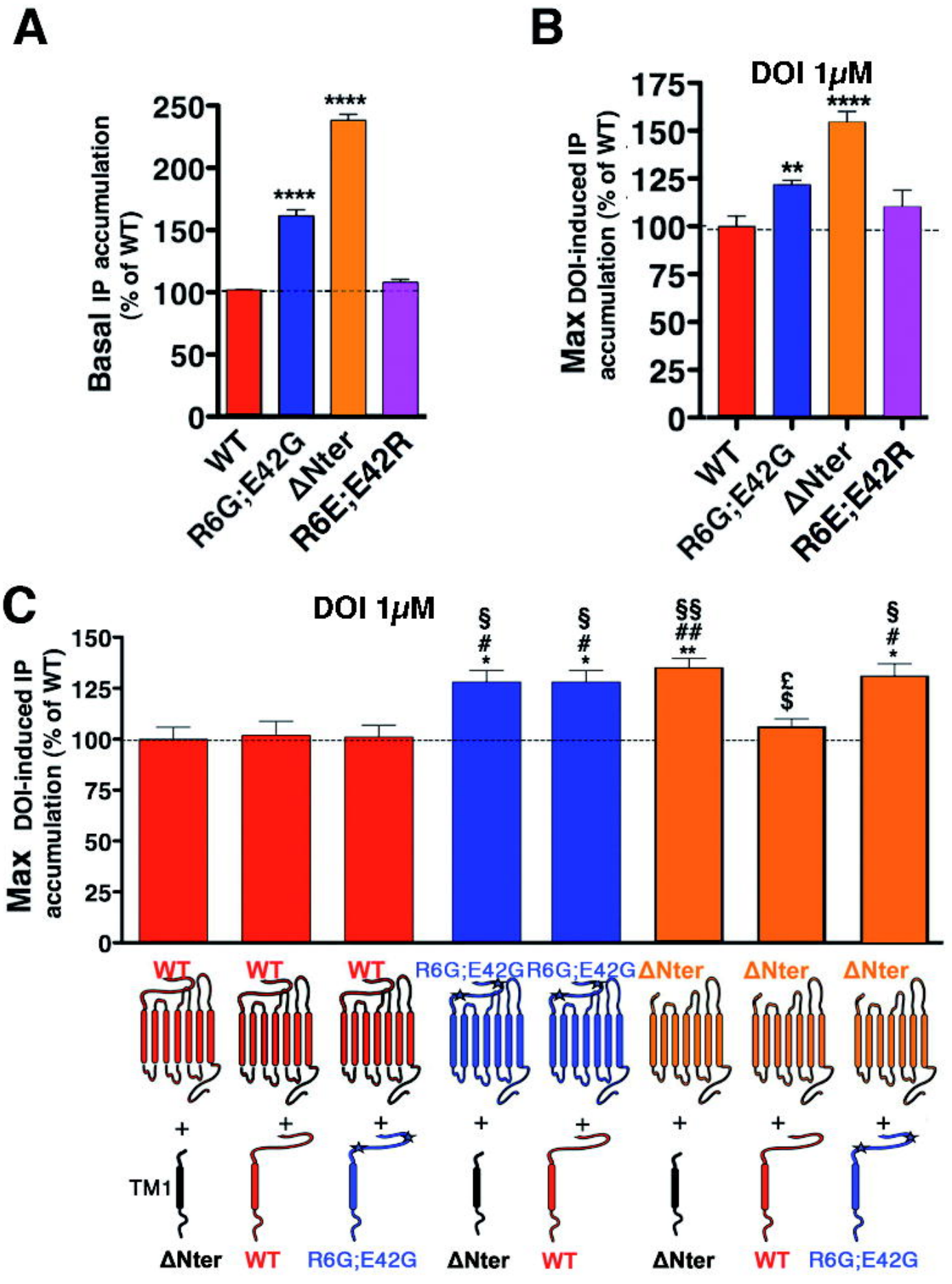
A
Basal IP accumulation (% of WT)
250
200
150
100
50
0
****
****
WT
R6G;E42G
ΔNter
R6E;E42R
B
DOI 1μM
Max DOI-induced IP accumulation (% of WT)
175
150
125
100
75
50
25
0
**
****
WT
R6G;E42G
ΔNter
R6E;E42R
C
DOI 1μM
Max DOI-induced IP accumulation (% of WT)
150
125
100
75
50
25
0
§ # *
§ # *
§§ ## **
£ $
§ # *
WT
WT
WT
R6G;E42G
R6G;E42G
ΔNter
ΔNter
ΔNter
+
TM1
ΔNter
WT
R6G;E42G
ΔNter
WT
ΔNter
WT
R6G;E42G

Figure 7

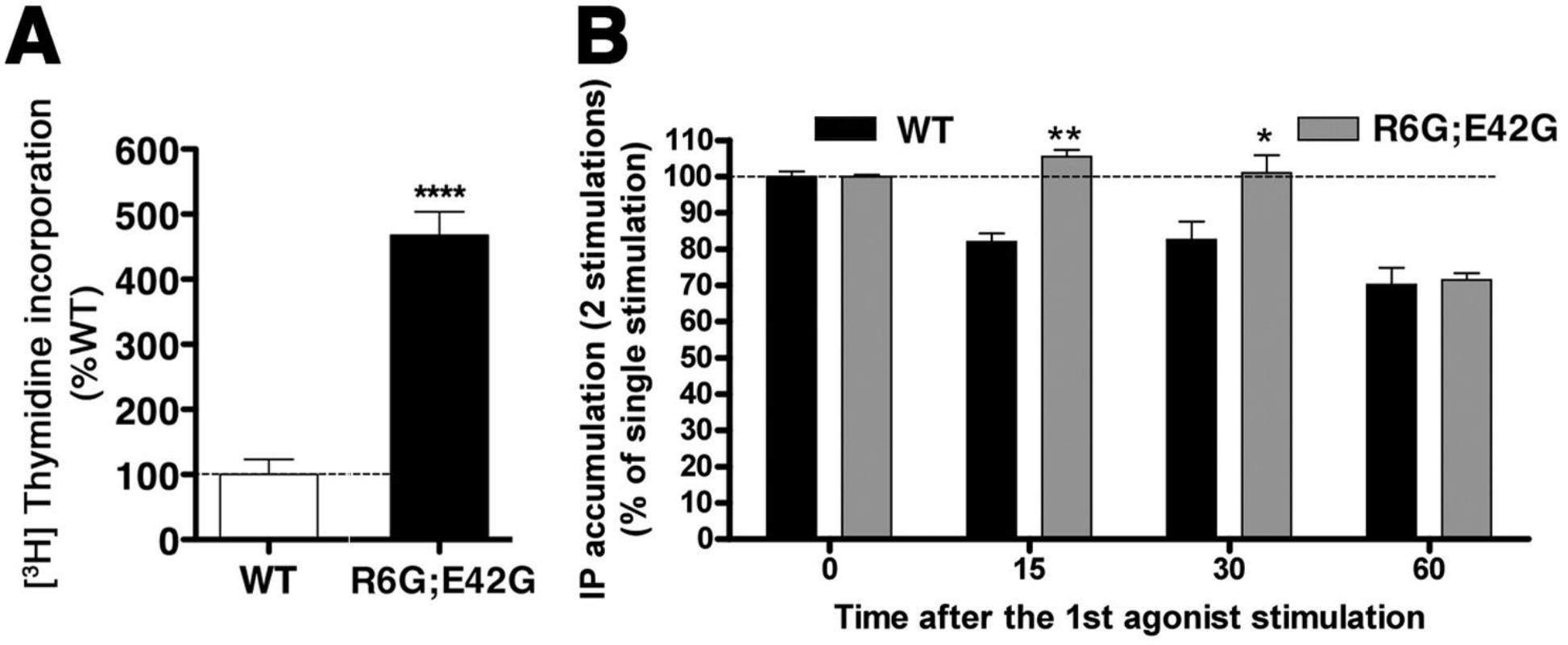
A
[3H] Thymidine incorporation (%WT)
600
500
400
300
200
100
0
****
WT
R6G;E42G
B
IP accumulation (2 stimulations) (% of single stimulation)
110
100
90
80
70
60
50
40
30
20
10
0
WT
R6G;E42G
**
*
0
15
30
60
Time after the 1st agonist stimulation